RESEARCH PAPER

Facile Fabrication of Co_3O_4 Nanostructures as an Effective Photocatalyst for Degradation and Removal of Organic Contaminants

Ali Abbasi [1], Mazyar Ahmadi Golsefidi [2], Mehdi Mohammad Beigi [2], Nazanin Sadri [2], Mehdi Abroudi [1]*

[1] *Young Researchers and Elite Club, Gorgan Branch, Islamic Azad University, Gorgan, Iran*

[2] *Department of chemistry, Faculty of sciences, Gorgan branch, Islamic Azad University, Gorgan, Iran*

ARTICLE INFO

Article History:
Received 10 October 2017
Accepted 21 December 2017
Published 01 January 2018

Keywords:
Co_3O_4
Methyl orange
Nanoparticle
Photocatalytic activity
Rhodamine B

ABSTRACT

Co_3O_4 nanoparticles were synthesized via a simple Co-precipitation reaction between precursors of cobalt and NH_3. The effect of different parameters such as concentration of NH_3 and precursors of cobalt on the size and photocatalytic activity of the products was investigated. The achieved nanoparticles were characterized by X-ray powder diffraction analysis, field emission scanning electron microscopy, energy-dispersive spectroscopy (EDS) and diffuse reflectance spectroscopy (DRS). The photocatalytic behavior of Co_3O_4 nanoparticles was evaluated using the degradation of various organic pollutants (rothamine B and methyl orange) under visible irradiation. Also effect of pH on the photocatalytic performance of Co_3O_4 nanostructures was investigated. Best concentration of NH_3 for degradation of methyl orange and rhodamine B is 3 mol, and most appropriate precursor of cobalt for the demolition of dyes is $Co(Hsal)_2$. Photo-degradation of Rhodamine B and methyl orange (89%) was performed using Co_3O_4 nanoparticle (band gap 1.7 eV) synthesized by $Co(Hsal)_2$ as precursor of cobalt under visible light irradiation for 4h.

How to cite this article
Abbasi A, Ahmadi Golsefidi M, Mohammad Beigi M, Sadri N, Abroudi M. Facile Fabrication of Co_3O_4 Nanostructures as an Effective Photocatalyst for Degradation and Removal of Organic Contaminants. J Nanostruct, 2018; 8(1): 89-96. DOI: 10.22052/JNS.2018.01.011

INTRODUCTION

Metal oxides are widely used in the various fields such as; heterogeneous catalysis, protein-purification systems [1], solar energy transformation, electronics devices and etc. Among the metal oxides, copper and cobalt are the most active for the decomposition of organic pollution [2, 3]. Cobalt oxide is one of the most important materials among the transition metal oxides and widely used in anode materials in gas and humidity sensors [4, 5], Li-ion rechargeable batteries, magnetism, and optical devices [6], catalyst for oxygen evolution and oxygen reduction reaction [7, 8], electrochemical capacitors for high power devices in energy storage systems (supercapacitors) [9, 10] and solar selective absorber, pigment for glasses and ceramics [11]. Also Co_3O_4 nanoparticles as additive has been used in various fields of material science such as improve temperature-stable $BaTiO_3$-based dielectrics [12]. Various methods have been applied for synthesis of metal oxides such as plasma sputtering [13], laser ablation technique, micro-emulsion [14], sol-gel route [15], spray pyrolysis [16], thermal salt

* *Corresponding Author Email: mahmadig@gmail.com*

decomposition [17], powder immobilization and hydrothermal method [18], that the majority of them are synthesized using water as a solvent [19, 20]. But among these methods, Co-precipitation method has been recognized as one of the important and accessible strategies for production of various nanoparticles, also this way has advantages compared to other routes including phase purity, high crystallinity and homogeneity of the materials synthesized.

Ellipsis of pollutants from water is a challenge for water treatment [21-23]. Amongst various ways for remove pollutants from water, photo-degradation has great importance. In these processes, organic structures decomposed by photo-catalyst material under UV or visible light and finally CO_2 and H_2O are achieved. The aim of the present work is study the effect of different concentration of NH_3 and various precursor of cobalt on the size and morphology of Co_3O_4 nanoparticles, and then studies obtained products in order to investigation of efficient photocatalyst. Here rhodamine B and methyl orange were used as organic pollution and sample 2 and 5 had the best photocatalytic activity.

MATERIALS AND METHODS

Cobalt (II) nitrate, acetylacetonate, NH_3, methanol Sodium salicylate (NaHsal) and salicylaldehyde (Sal) were purchased from Merck and used without purification. Deionized water was used as solvent. The prepared Co_3O_4 samples were characterized using X-ray diffractometer using Ni-filtered Cu Kα radiation, scanning electron microscope (SEM), model 1455VP. Prior to taking images, the samples were coated with a very thin layer of Pt to make the sample surface conducting and prevent charge accumulation. Also UV-vis spectrum of the sample was taken on a UV-vis spectrophotometer (Shimadzu, UV-2550, Japan) + visible sources of 400 W Osram lamps.

Synthesis of Co_3O_4

Co_3O_4 samples were prepared by using various precursor of Cobalt (II), NH_3 and de-ionized water as solvent. First 1 mol of various precursor of Cobalt dissolved in deionized water then NH_3 as alkaline agent was added to solution. The obtained precipitates were collected, washed and dried at 60 °C, then calcinated at 450 °C for 2 h. The production conditions of Co_3O_4 nanostructures were summarized in table 1.

syntheses of various precursors

For the synthesis of various precursors, 0.4mol cobalt (II) nitrate dissolved in methanol then 0.8 mol acetylacetonate was added to above solution at 60°C. The obtained precipitates were washed and dried. For the synthesis of $Co(Sal)_2$ and $Co(Hsal)_2$, in above method salicylaldehyde and Hsal (salicylate) were replaced to acetylacetonate.

Photocatalytic measurements

The photocatalytic performance of the as-synthesized Co_3O_4 nanostructures was evaluated by applying of the various contaminants solution. 0.05 g Co_3O_4 nanoparticles were used for demolition of 40 ml dye solution (10 ppm) then solution was mixed by a magnet stirrer for 1 h in darkness. The solution was irradiated by a 400 W visible lamp which was placed in a quartz vessel in a reactor. After each 20 minutes, sampling (about 5-10 ml) was performed and was centrifuged to separate the catalyst and then was analyzed with the UV–Vis spectrometer.

RESULTS AND DISCUSSION

Co_3O_4 nanostructure is characterized by X-Ray Diffraction Analysis (XRD), Energy Dispersive analysis of X-rays (EDS), Diffuse Reflectance Spectroscopy (DRS) and Scanning Electron Microscopy (SEM).

Fig. 1 present the XRD patterns of the Co_3O_4 powder with different precursor of cobalt. The X-ray diffractograms were scanned between 2

Table 1. The reaction conditions for synthesis of Co_3O_4 via co-precipitation method

Sample	Alkaline agent	Ratio of ammonia	Ligand (capping agent)	Figure of SEM
1	NH_3	1	_	3a and b
2	NH_3	3	_	3c and d
3	NH_3	3	Acetylacetonate	4a and b
4	NH_3	3	Salicylaldehyde	4c and d
5	NH_3	3	Sodium salicylate	4e and f

angles of 15-75°. Each spectrum indicate the peaks characteristic for the Co_3O_4 crystal with 2 values of ~ 19°, 31.1°, 36.9°, 38.5°, 45°, 55.8°, 59.5° and 65.3° that the related to h k l planes of (1 1 1), (2 2 0), (3 1 1), (2 2 2), (4 0 0), (4 2 2), (5 1 1) and (4 4 0), respectively. The XRD spectra of as-prepared Co_3O_4 nanoparticles were demonstrated a pure cubic phase (space group: Fd-3m) which was quite close to the literature amounts (JCPDS No. 76-1802). It can be seen that the highest intensity of the diffraction peak for all powders is (3 1 1) and crystallite size, by using the Scherrer equation and full with at half maximum (FWHM) was obtained about 30 nm.

To confirm the chemical composition of the synthesized powders, the sample was examined by EDS analysis (Fig. 2). This spectrum confirms that the targeted chemical composition could achieve in the final product. Obviously, the sample is composed of Co and O.

The effect of concentration of NH_3 on the particle size was investigated. The various amount of NH_3 (1 and 3 mol that were named sample 1, 2) as alkaline agent were used for study effect of concentration on the particle size. As can be seen by increasing concentration of NH_3 to 3 mol, particle size was decreased (Fig. 3c and d) compared to concentration of 1 mol (Fig. 3a and

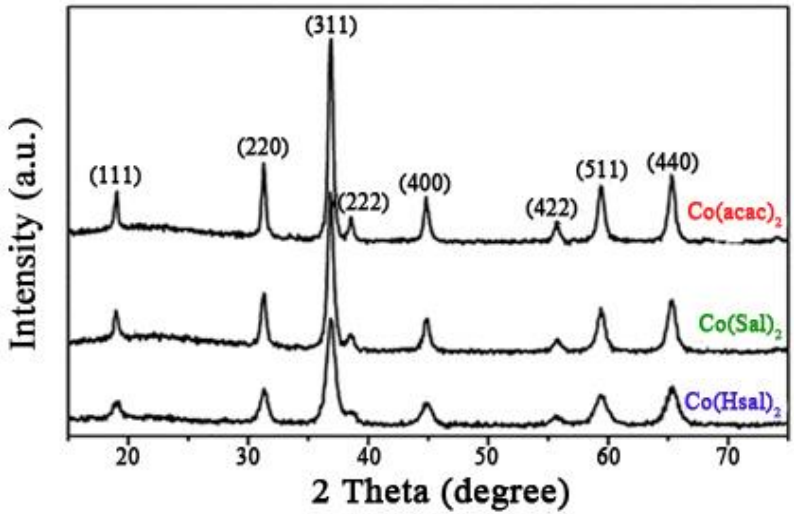

Fig. 1. XRD patterns of Co_3O_4 produced by Co-precipitation method.

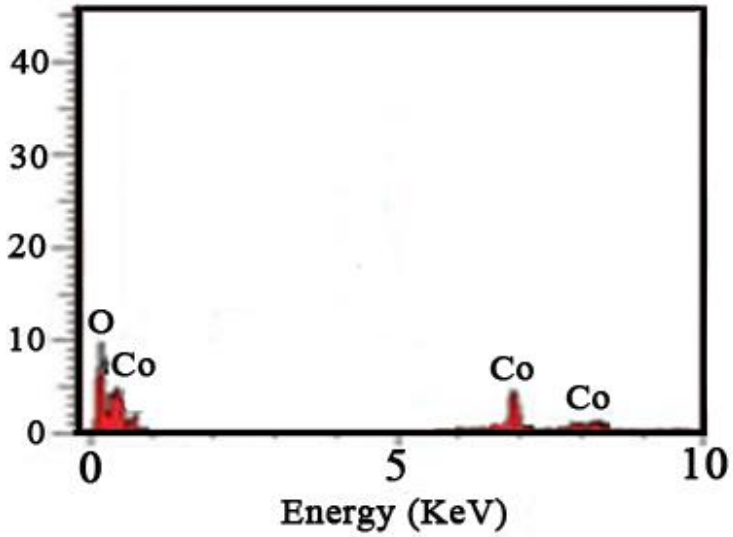

Fig. 2. EDS curve of Co_3O_4 nanostructure (sample 5)

b). In the next step, for the investigate the effect of ligand, were used of $Co(acac)_2$, $Co(Sal)_2$ and $Co(Hsal)_2$ as various precursors of cobalt (samples 3, 4 and 5 respectively). Based on the FESEM micrographs of the Co_3O_4 samples prepared with the aid of different capping agents (Fig. 4a-f), it is suggested that Hsal has a great impact on the preparation of uniform spherical Co_3O_4 nanostructures. As it can be seen in Fig. 4 e and f nanoparticles synthesized by $Co(Hsal)_2$ are very uniform compared to nanoparticles prepared with $Co(acac)_2$ (Fig. 4a and b) and $Co(Sal)_2$ (Fig. 4c and d). Hence, the use of Hsal is favourable to form uniform spherical Co_3O_4 nanostructures.

The photocatalytic activity of a material is controlled by absorption coefficient and optical band gap that which these features are related to the electronic structure of the material. Fig. 5 shows the UV–Vis absorption spectrum of the Co_3O_4 nanoparticles. In this spectrum can be seen the absorption peaks at 207, 245 and 385 nm.

The band gap of nanoparticles was determined by Diffuse Reflectance spectroscopy (DRS) that estimated by Tauc's equation;

$$\alpha = \alpha_0 (hv - Eg)^n / hv \quad (1)$$

where α is absorption coefficient, hν is the photon energy, Eg is the optical band gap, α_0 and h are the constants and n related to the type of electronic transition and can have any value between 0.5 to 3 eV. The energy gap (Eg) of the sample was determined by extrapolating the linear section of the plots of $(\alpha h\upsilon)^2$ vs. hυ to the energy axis (1.7 eV) as show in Fig. 6, in result the nanoparticles are photoresponsive in the visible ranges, and as has been shown, Co_3O_4 has absorption in the visible area.

The photo-catalytic activities of the Co_3O_4 nanoparticles were measured by monitoring the degradation of rhodamine B and methyl orange in an aqueous solution under visible irradiation. In this section was surveyed the effect of various parameters including; kind of pollutant, particle size and pH on the photocatalytic activity of nanostructures. As depicted in Fig. 7, after applying visible irradiation, a photon produce electron and hole in the conduction band (CB) and valence band (VB) of Co_3O_4, respectively.

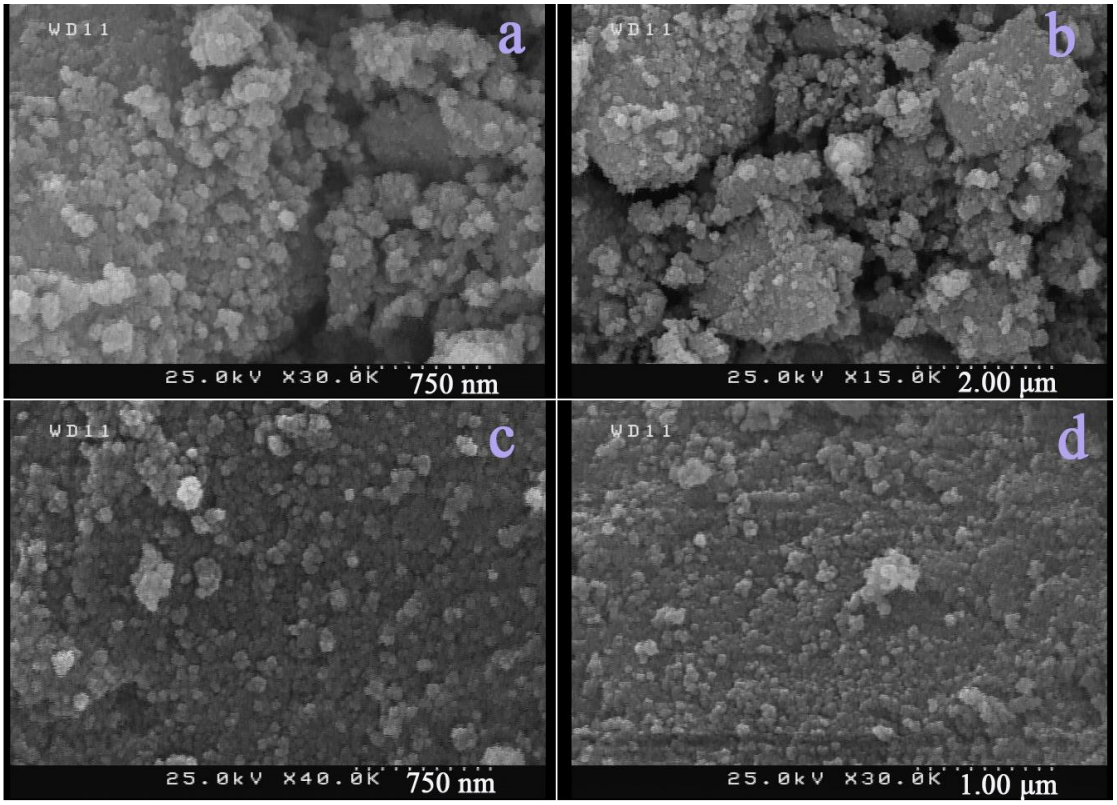

Fig. 3. SEM images of Co_3O_4 prepared in various concentrations of NH_3; (a and b) 1 mol, (c and d) 3 mol.

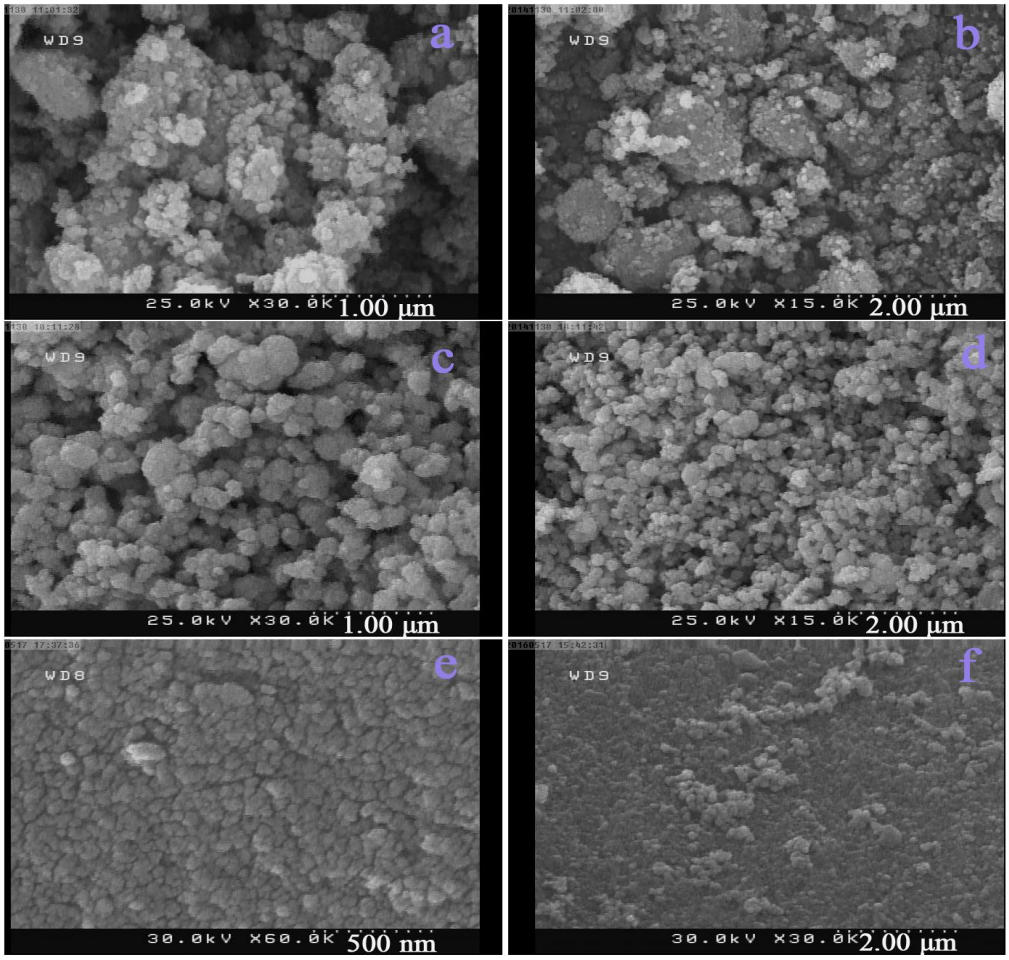

Fig. 4. SEM images of Co_3O_4 prepared by (a and b) $Co(acac)_2$, (c and d) $Co(Sal)_2$ and (e and f) $Co(Hsal)_2$.

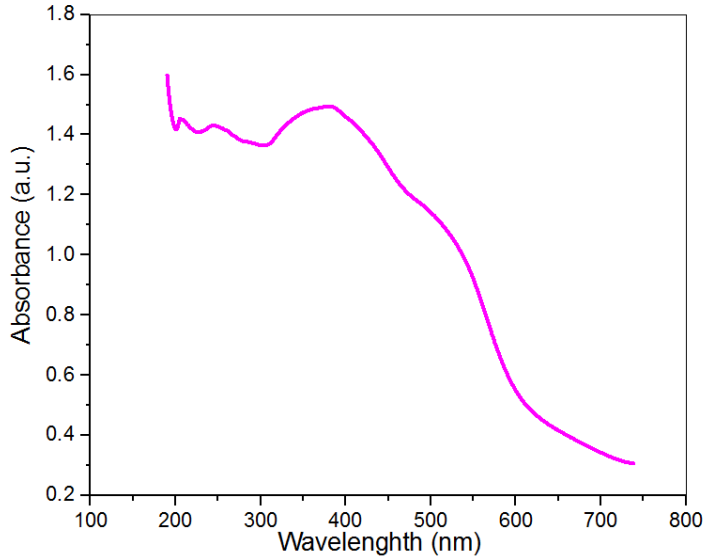

Fig. 5. UV–Vis diffuse reflectance spectrum of Co_3O_4 (sample 5)

The rhodamine B and methyl orange demolition percentage in time of t (DP (t)) were calculated as follows:

$$DP(t) = \frac{A_0 - A_t}{A_0} \times 100 \quad (2)$$

Where A_t and A_0 are the absorption value of the solution at 0 and t minute [24-28].

The presented mechanism of the demolition of pollutants can be displayed as:

$$Co_3O_4 + h\nu \rightarrow Co_3O_4^{*} + e^{-} + h^{+}$$

$$h^{+} + H_2O \rightarrow OH^{\cdot}$$

$$2e^{-} + O_2 + 2\,H^{+} \rightarrow O_2^{-\cdot}$$

$$OH^{\cdot} + O2^{-\cdot} + \text{pollutants} \rightarrow \text{Degradation products}$$

No dye demolition after 60 min without using visible light irradiation or nanocatalysts. Hence, the degradation efficiency of methyl orange and

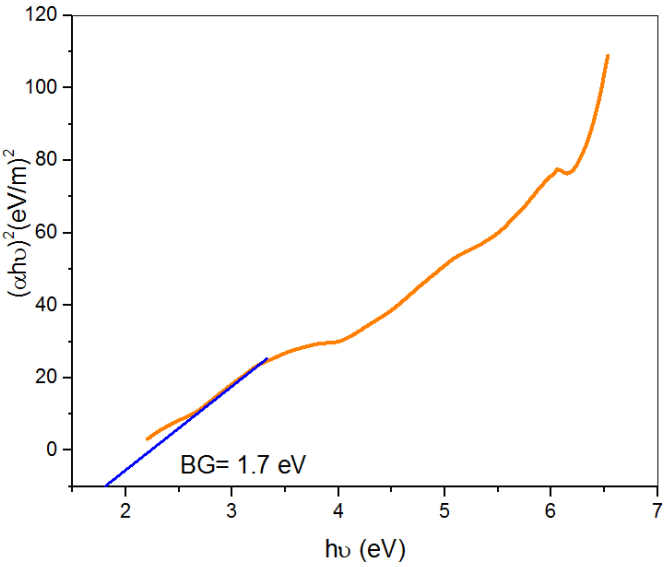

Fig. 6. Plot to determine the band gap of produced Co_3O_4 (sample 5).

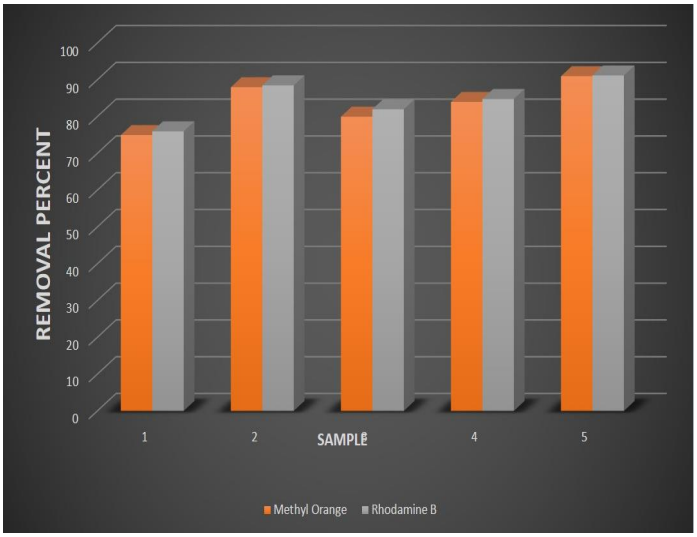

Fig. 7. Photodegradation of methyl orange and rhodamine B by Co_3O_4 nanoparticles

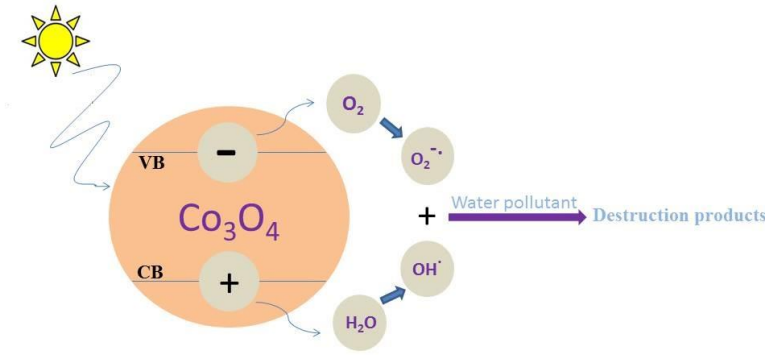

Fig. 8. Schematic diagram of the reaction mechanism of organic pollutants photodegradation by Co_3O_4

rhodamine B by Co_3O_4 nanoparticles produced with different concentration of NH_3 and various precursors of cobalt is determined as shown in Fig. 7 under visible light irradiation. Also the irradiation time was 4 h. In the case of methyl orange pH was adjusted at 5, while pH for rhodamine B was 7. Since the methyl orange is an anionic combination, as result decreasing pH value results in a higher adsorption amount of methyl orange on the photocatalyst surface. As shown in Fig. 8, in acidic condition the surface of nanostructure is covered by more positive charge and subsequently anionic molecules can be more adsorbed on the surface. The most appropriate samples for demolition of rhodamine B were achieved sample 2 and sample 5 with demolition percentage~ 87% and 89% respectively. The most appropriate samples for degradation of methyl orange were achieved sample 2 and sample 5 with demolition percentage ~ 86% and 89% respectively. Sample 2 and 5 have higher surface area duo to smaller particle size. Therefore more dye molecules are affected in same time. With the decrease of particle size, the ratio of surface area to volume increases, therefore the catalytic performance is better.

CONCLUSION

Co_3O_4 nanostructures were prepared by a Co-precipitation process at room temperature. The effects of concentration and precursors of cobalt were studied and for optimization size, after completing each step, SEM analyses were taken from the produced nanoparticles. The influence concentration of NH_3 and precursors of cobalt on the photocatalytic properties Co_3O_4 nanoparticle was studied. Hereon was used of rhodamine B and methyl orange as organic pollutants. Results indicated that the best concentration of NH_3 for destruction of methyl orange and rhodamine B was achieved 3mol, and most appropriate precursor of cobalt for the demolition of dyes was achieved $Co(Hsal)_2$.

ACKNOWLEDGEMENTS

The authors are grateful to Islamic Azad University (IAU) for providing financial support to undertake this work.

CONFLICT OF INTEREST

The authors declare that there are no conflicts of interest regarding the publication of this manuscript.

REFERENCE

1. Murawski L. Chung C. H, Mackenzie J. D, Electrical properties of semiconducting oxide glasses, J Non-Cryst Solids., 1979; 32; 91.
2. Ciocilteu S. M, Salou M, Kiyozumi Y. H, Niwa S, Mizukamia F, Haneda M, Uniform distribution of copper and cobalt during the synthesis of SiMFI-5 from kanemite through solidstate transformation, J. Mater. Chem., 2003; 13: 602.
3. Mhamdi M, Khaddar-Zine S, Ghorbel A, Influence of the Co/Al ratio and the temperature of thermal treatment on cobalt speciation and catalytic properties of Co-ZSM-5 prepared by solid-state ion exchange, Appl Catal A-Gen, 2008; 337: 39.
4. Grisel R. J. H, Nieuwenhuys B. E, Selective Oxidation of CO, over Supported Au Catalysts, J. Catal., 2001; 199: 48.
5. Ando M, Kobayashi T, Iijima S, Haruta M, Optical recognition of CO and H2 by use of gassensitive Au–Co3O4 composite films, J.Mater. Chem., 1997; 7: 1779.
6. Roth W. L, The magnetic structure of Co3O4, J. Phys. Chem. Solids, 1964; 25: 1.
7. Seike T, Nagai J, Electrochromism of 3d transition metal oxides, Sol. Energy Mater. 1991; 22: 107.
8. Kadam L. D, Patil P. S, Thickness-dependent properties of sprayed cobalt oxide thin films, Mater. Chem. Phys. 2001; 68: 225.

9. Wang S, Zhang B, Zhao C, Li S, Zhang M, Yan L, Valence control of cobalt oxide thin films by annealing atmosphere, Appl Surf Sci. 2011; 257: 3358.
10. Kim H. K, Seong T. Y, Lim J. H, Cho W. L, Yoon Y. S, Electrochemical and structural properties of radio frequency sputtered cobalt oxide electrodes for thin-film supercapacitors, J. Power Sources, 2001; 102: 167.
11. Barreca D, Massignan C, Daolio S, Fabrizio M, Piccirillo C, Armelao L, Tondello E, Composition and Microstructure of Cobalt Oxide Thin Films Obtained from a Novel Cobalt(II) Precursor by Chemical Vapor Deposition, Chem. Mater. 2001; 13: 588.
12. Hideywki K, Motomasa I, Effects of SiO2 and Cr_2O_3 on the formation process of ZnO varistors, J. Mater. Sci. 1988; 23: 4379.
13. Shinde V. R, Mahadik S. B, Gujar T. P, Lokhande C. D, Supercapacitive cobalt oxide (Co_3O_4) thin films by spray pyrolysis, Appl. Surf. Sci. 252 (2006) 7487.
14. Dasilva L. M, Boodts J. F. C, Faria L. A. D, Oxygen evolution at RuO_2(x) + Co_3O_4 (1-x) electrodes from acid solution, Electrochim Acta, 2001; 46: 1369.
15. Jiang S. P, Tseung A. C. C, Homogeneous and heterogeneous catalytic in cobalt oxide / graphite air electrodes, J. Electrochem. Soc. 1990; 137: 764.
16. Mousavand T, Takami S, Umetsu M, Ohara S, Adschiri T, Supercritical hydrothermal synthesis of organic-inorganic hybrid nanoparticles. J. Mater. Sci. 2006; 41: 1445.
17. Vidal-Vidal J, Rivas J, LópezQuintel M. A, Synthesis of monodisperse maghemite nanoparticles by the microemulsion method, Colloids Surf. A, 2006; 288: 44.
18. Takeshi T, Hamagamia T, Kawamurab T, Yamaki J, Tsuji M, Laser ablation of cobalt and cobalt oxides in liquids: influence of solvent on composition of prepared nanoparticles. Appl. Surf. Sci. 2005; 243: 214.
19. Yuan Z, Huang F, Feng C, Sun J, Zhou Y, Synthesis and electrochemical performance of nanosized Co_3O_4, Mater. Chem. Phys. 2004; 79: 1.
20. Yang H, Hu Y, Zhang X, Qiu G, Mechanochemical synthesis of cobalt oxide nanoparticles. Mater. Lett. 2004; 58: 387.
21. Llusar M, Royo V, Badenes J. A, Tena G, Monros G, Nanocomposite Fe_2O_3–SiO_2 inclusion pigments from post-functionalized mesoporous silicas, J. Eur. Ceram. Soc. 2009; 29: 3319.
22. Reddy M. V, Yu T, Sow C. H, Shen Z. X, Lim C. T, Rao C. V. S, Chowdari B. V. R, α-Fe_2O_3 Nanoflakes as an Anode Material for Li-Ion Batteries, Adv. Funct. Mater. 2007; 17: 2792.
23. Wu P. C, Wang W. S, Huang Y. T, Shen H. S, Lo Y. W, Tsai D. B, Shieh D. B, Yeh C. S, Porous Iron Oxide Based Nanorods Developed as Delivery Nanocapsules, Chem. Eur. J. 2007; 13: 3878.
24. Abbasi A, Ghanbari D, Hamadanian M, Salavati-Niasari M, Photo-degradation of methylene blue: Photocatalyst and magnetic investigation of Fe_2O_3-TiO_2 nanoparticles and nanocomposites, J Mater Sci: Mater Electron. 2016; 27: 4800.
25. Abbasi A, Khojasteh H, Hamadanian M, Salavati-Niasari M, Synthesis of $CoFe_2O_4$ nanoparticles and investigation of the temperature, surfactant, capping agent and time effects on the size and magnetic properties, J Mater Sci: Mater Electron. 2016; 27: 4972-4980.
26. Abbasi A, Hamadanian M, Salavati-Niasari M, Mortazavi-Drazkollah S, Facile size-controlled preparation of highly photocatalytically active $ZnCr_2O_4$ and $ZnCr_2O_4$/Ag nanostructures for removal of organic contaminants, J. Colloid Interface Sci., 2017; 500: 276-284.
27. Mortazavi-Derazkola S, Salavati-Niasari M, Amiri O, Abbasi A, Fabrication and characterization of Fe_3O_4@SiO_2@TiO_2@Ho nanostructures as a novel and highly efficient photocatalyst for degradation of organic pollution, Journal of Energy Chemistry, 2017; 26: 17-23.
28. Khojasteh H, Salavati-Niasari M, Abbasi A, Azizi F, Enhessari M, Synthesis, characterization and photocatalytic activity of PdO/TiO_2 and Pd/TiO_2 nanocomposites, J Mater Sci: Mater Electron. 2016; 27: 1261-1269.